Available online at www.sciencedirect.com

ScienceDirect

ARTICLE

Ti(C, N, O) Nanocomposite Films Fabricated by Filtered Cathodic Vacuum Arc Using CO_2 and N_2 as Precursors

Hou Qingyan,   Shen Yongqing,   Fu Kaihu,   Zhou Han,   Ying Minju,   Zhang Xu,   Liao Bin

Key Laboratory of Beam Technology and Modification of Ministry of Education, Beijing Normal University, Beijing 100875, China

Abstract: Ti(C,N,O) films were deposited on Si(100) and 304 stainless steel by Filtered Cathodic Vacuum Arc (FCVA) using CO_2 and N_2 (with ratio of 1:1) as precursors. The effect of gas flow rate on the composition, phase structure and properties of films was investigated by XPS, XRD, Raman, SEM, tribological test and electrochemical workstation. Results show that the contents of C and N increase obviously, while contents of O and Ti decrease slightly as the gas flow rate increases from 10 mL/min to 50 mL/min. The contents of C and N decrease, while content of Ti increases slightly and content of O increases dramatically as the gas flow rates from 50 mL/min to 80 mL/min. The phase structure of Ti(C,N,O) films transformes from nc-Ti(C,N,O) nanocrystal structure to nc-Ti(C,N,O)/a-CN_x nanocomposite structure, a-TiO_2/a-CN_x and N-doped a-TiO_2/a-C nanocomposite structure with gas flow rate increasing from 10 mL/min to 80 mL/min. The N-doped a-TiO_2/a-C nanocomposite showed the lowest friction coefficient. Both nc-Ti(C, N, O)/a-CN_x nanocomposite structure and N-doped a-TiO_2/a-C nanocomposite structure show good anticorrosion ability in Hanks balance solution.

Key words: Ti(C,N,O); filtered arc; CO_2; corrosion; nanocomposite

Hard ceramic coatings such as titanium nitride (TiN), and titanium carbide (TiC) have been extensively studied because of their excellent properties. Due to the excellent properties in high hardness, low Young's modulus, low friction, good corrosion resistance, good thermal conductivity, high electric conductivity and melting temperature, Titanium carbonitride TiCN films have already been widely used in cutting tools and medical fields[1-3]. As well known that, the affinity of O toward Ti is high, the introduction of O into Ti-C-N ternary system will cause a series of phase transition in films, which will offer a wide range variation of properties[4]. Titanium oxycarbonitride films have been studied as decorative materials with narrow color range (black)[4]. Various methods have been used to prepare titanium oxycarbonitride films, including magnetron sputtering and chemical vapor deposition[4,5]. Filtered Cathodic Vacuum Arc (FCVA) technique, with high ionization rate, high ion drift energy and free of macro-particle contamination, has been used as an excellent method for preparing compact, smooth and uniform films. In our previous work, nc-ZrCN/a-CN_x and nc-TiC/a-C nanocomposite films were successfully prepared by FCVA technique [6,7]. Due to the rare application of FCVA technique in preparation of titanium oxycarbonitride films, the unique properties of titanium oxycarbonitride films prepared by FCVA technique are attractive for investigation. Furthermore, CO_2 and N_2 gas mixture is seldom used together as precursors, and their effect on the preparation of films is expected to be studied. And the inertness of both CO_2 and N_2 also makes a safe process of films preparation and simplifies the procedure of titanium oxycarbonitride films preparation.

In this paper, Ti(C, N, O) films were fabricated by FCVA using CO_2 and N_2 as reactive gas (with ratio of 1:1). The

compositional, structural, frictional and anticorrosion properties of Ti(C, N, O) films were studied as gas flow rate varies from 10 mL/min to 80 mL/min.

1   Experiment

The schematic diagram of FCVA system is shown in Fig.1. Ti(C,N,O) films were deposited on Si(100) and 304 SS by FCVA technique. Cathode was a titanium plate with 90 mm in diameter and 99.99% in purity, which was applied as plasma source. The triggered titanium plasma was guided into a 90 ° curving duct with wrapped solenoid coils outside, through which the unwanted macro-particles were filtered. Prior to deposition, the substrates were sputtered for 20 s under –800 V bias, which can improve the adhesion between films and substrates. Then CO_2 and N_2 gas mixture (1:1) was injected in vacuum chamber to collide with almost fully ionized Ti plasma, and new plasma was guided to impinge toward substrates. The substrates were positioned vertically toward the exit of filtered duct at 10 cm distance. The experimental parameters are shown in Table 1. The surface images of films were pictured by SEM (Hitachi S-4800). Elemental composition and chemical bonds were estimated by X-ray photoelectron spectroscopy (Thermo Fisher ESCALAB250 system). The crystal structure of films was measured by glancing angle (1 °) X-ray diffraction (XRD) measurement (D/2500H with Cu Kα radiation, operating at 40 kV, 200 mA) within 2θ range of 30 °~80 °. The average grain size of film (D) was calculated from the full width at half maximum (FWHM) using Scherrer's formula:

$$D = \frac{k\lambda}{B\cos\theta} \qquad (1)$$

where, k=0.89, B is the FWHM, λ is the wavelength, and θ is the diffraction angle. Raman spectra were acquired with Jobin-Yvon HR800 monochromator and a nitrogen cooled CCD at 7 mW power. The 532 nm line of an Ar-Kr laser was used to produce excitation light and the scanning range was limited 1000~2000 cm^{-1}. The thickness and curvature of films were measured by the surface morphology device (Talysurf 5P-120, Rank Taylor Hobson, United Kingdom). Internal compressive stress was calculated on radius change of curvature of the wafer, before and after deposition. The Stoney formula was used to estimate the internal stress, which is given as:

$$\delta = \frac{1}{6} \cdot \frac{E_s t_s^2}{(1-\upsilon_s)t} \cdot (\frac{1}{R_n} - \frac{1}{R_0}) \qquad (2)$$

where, E_s, v_s, t_s, t are Young's elastic modulus (GPa), Poisson ratio, thickness of Si wafer (mm) and thickness of films, respectively. Tribological property was obtained by Rotating Tribological Test with Si_3N_4 balls under 1 N, 200 r/min for 10 min, at room temperature with a humidity of 22%. The friction coefficient was average of four testing data of different areas on one film. Electrochemical behavior was performed using CS300 electrochemical workstation at 37 ℃ Hanks balanced salt solution to simulate the human body fluid environment (Solarbio commercial Hank's Balanced Salt Mixture). A conventional three electrodes system was used, in which the films deposited on 304 SS substrates were employed as the working electrode (exposed area 0.5 cm^2), a platinum coil as auxiliary electrode and a saturated calomel electrode (SCE) as reference electrode. Potentiodynamic polarization tests were performed at a scan rate of 5 mV/s.

2   Results and Discussion

2.1   Elemental composition and surface images

The elemental composition of Ti, O, N and C as a function of gas mixture flow rate are shown in Fig.2. The contents of C and N increase obviously, while contents of O and Ti decrease slightly with the gas flow rate increasing from 10 to 50 mL/min. When gas flow rate increases, the O, N
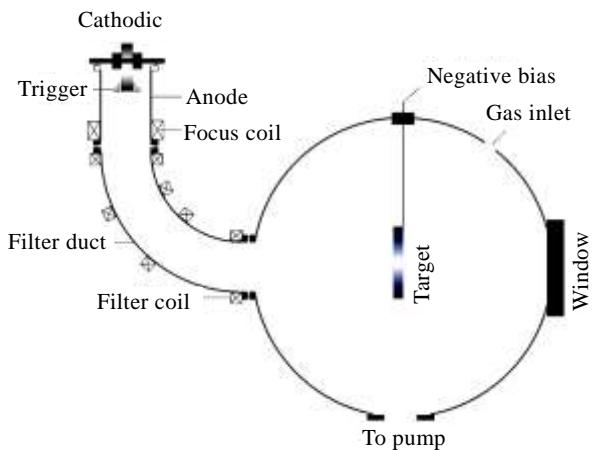

Fig.1   Schematic diagram of filtered cathodic vacuum arc deposition system

Table 1   Deposition parameters used for the preparation of Ti(C,N,O) films

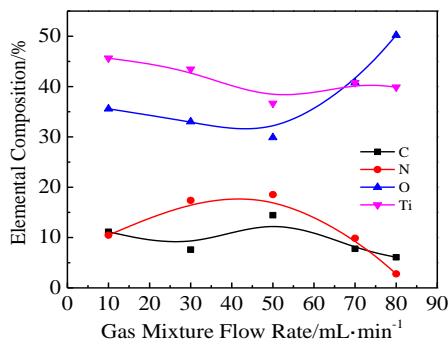| Gas mixture flow rate/ mL·min^{-1}	Ti(C,N,O) films thickness/nm	Gas pressure/Pa	Substrate bias/V	Deposition time/min	Crystal size/nm
10	342	1.1×10^{-2}	-200	10	6.4 (111)Ti(C,N,O)
30	301	3.1×10^{-2}	-200	10	8.2 (111)Ti(C,N,O)
50	365	4.7×10^{-2}	-200	10	12.5 (111) Ti(C,N,O)
70	200	1.2×10^{-1}	-200	10	-
80	270	4.7×10^{-1}	-200	10	-

Fig.2　Elemental composition of films deposited under different CO_2 and N_2 gas mixture flow rates

and C plasma densities ionized by colliding with Ti plasma (consisted of Ti^+, Ti^{2+}, Ti^{3+}, generally, Ti^{2+} is dominated [8]) increase; therefore more N and C element deposit in the films. Ti plasma is strongly cooled by collisions and with carbon dioxide and nitrogen gas, mean energy of Ti plasma decreases with gas pressure increases. The decrease of O may be caused by less C and N element is preferentially sputtered by lower mean energy Ti plasma at higher gas flow rate. The contents of C and N decrease obviously, while contents of Ti increase slightly and contents of O increase dramatically as the gas flow rate increases from 50 mL/min to 80 mL/min. The increase of O content and the decrease of C and N contents at higher gas flow rate may be related to the ionization and dissociation possibility of CO_2 and N_2 gas interacted with Ti plasma, as the mean energy of Ti plasma decreases remarkably when it is collided with gas molecules under higher gas pressure and may be lower than dissociative energy or the first ionization energy. The first ionization energy (13.62 eV) and dissociative energy (one side of O=C=O: 7.76 eV) of O element are lower than those(first ionization energy N 14.53 eV and dissociative energy N≡N: 9.79 eV) of N element. The first ionization energy (13.62 eV) of O element is higher than that of C element (C 11.26 eV), but the dissociative energy of O element (one side of O=C=O: 7.76 eV) is much lower

than that of C element (O=C=O:15.52 eV). Therefore O element is more likely to be ionized or dissociated by lower mean energy of Ti plasma at higher gas flow rate than N element and C element.

The surface images of Ti(C,N,O) films deposited under different gas flow rates are shown in Fig.3. As shown in Fig.3a and Fig.3b, films deposited under 10 and 50 mL/min gas flow rate are uniform and smooth, and it may be associated with the bombardment of Ti plasma with higher energy under low gas pressure, which can compact films. The surface morphology of film deposited under 80 mL/min gas flow rate shows light and shade tracts, which indicate a relatively rough surface morphology, and the reason might be the lower energy of Ti plasma under high gas pressure has little bombardment effect on films surface.

2.2　Structure analysis

2.2.1　XPS results

X-ray photoelectron spectroscopy is a common method in chemical bonds analysis of film. To diminish the contamination of O, C and N, Ti(C, N, O) films were sputtered by Ar^+ for 20 s. The XPS patterns of Ti 2p are presented in Fig.4a, the binding energy 454.5 eV of Ti $2p_{3/2}$ is ascribed to the mixture of TiC, TiN and TiO because of their close binding energy [9]. Ti^{4+}(458.5 eV) represents Ti-O bonds of TiO_2. The binding energy 456.5 eV is related to the O preferential sputtering of TiO_2 by Ar^+ or the Ti(C, N, O) compound[10,11]. It's clear that the peak of TiC, TiN and TiO decreases and eventually disappears, whereas, the peaks of TiO_2 increases as gas flow rate increases from 10 mL/min to 80 mL/min. The Ti spectra transform from Ti-(C, N, O) bonds dominant to TiO_2 bonds dominant. C1s spectra of films are presented in Fig.4b. There is a strong C-Ti peak (281.8 eV) in film under 10 mL/min gas flow rates; as gas flow rate increases to 30 mL/min, C-Ti peak decreases dramatically. As the gas flow rate increases to 50 mL/min, C-Ti peak disappears. There are C-C peaks (284.8 eV) in all films. C-N peaks (287.0 eV) exist in films under 50 and 70 mL/min. C-O peak (290.0 eV) only exists in film under 80 mL/min gas flow rate. As shown in Fig.4c, N-Ti peaks (396.5 eV) exist in films between 10 and 70 mL/min gas flow rate, and the N-C peaks exist in films under 50 and 70 mL/min

Fig.3　SEM images of Ti(C,N,O) films deposited under different gas mixture flow rates: (a) 10 mL/min, (b) 50 mL/min, and (c) 80 mL/min
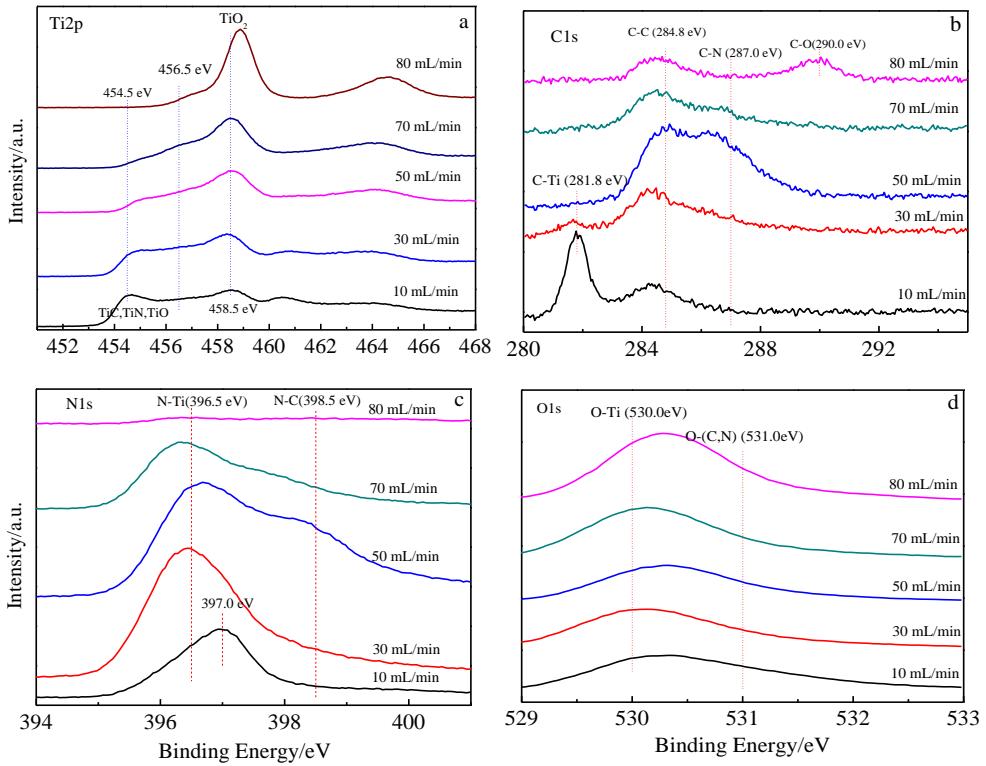
Fig.4　XPS spectra of Ti 2p (a), C 1s (b), N 1s (c) and O 1s (d) of the films deposited under different CO_2 and N_2 gas mixture flow rate

gas flow rate, which agrees well with the C-N peaks in C 1s spectra. There is not any peak under 80 mL/min gas flow rate. The peak at 397.0 eV in film deposited under 10 mL/min gas flow rate is possibly the N atoms in intergranular or interstitial space of solid solution. The O 1s XPS spectra of films (Fig.4d) can be separated into two parts, O-Ti bonds (~ 530.0 eV) and O-(C,N) bonds(~531.0 eV).

2.2.2　XRD results

　The structural evolution of the Ti(C, N, O) films as a function of gas flow rate is presented in Fig.5. The XRD patterns reveal a strong dependence of film structure on gas flow rate. It can been seen that films deposited under low gas flow rate (≤50 mL/min) show face centered cubic (fcc) structure, which are confirmed by the appearance of three main diffraction peaks, (111), (220) and (311) planes. Due to the same crystallographic structure and close lattice parameters of TiC, TiN and TiO (a_{TiO}=0.4117 nm, PDF#08-0117; a_{TiN}=0.4240 nm, DF#06-0642; a_{TiC}=0.4328 nm, PDF#05-0693), it's difficult to distinguish the TiC, TiN and TiO from XRD patterns. The positions of XRD peaks (111), (220), (311) are between TiC, TiN and TiO, and a solid solution-type Ti(C,N,O) can be imaged, where all or some of C, O and N atoms share the same cubic lattice. There is a strong (111) preferential orientation, its intensity keeps rising with gas mixture flow rate increasing from 10 mL/min to 50
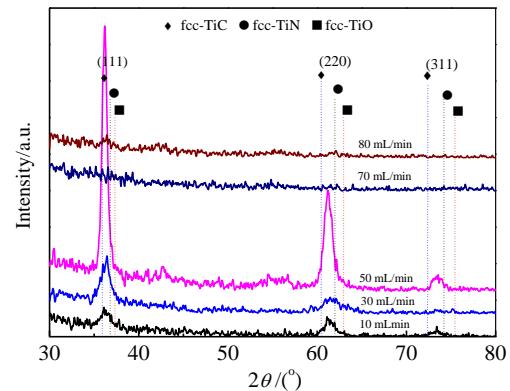

Fig.5　XRD patterns of films deposited under different CO_2 and N_2 gas mixture flow rate

mL/min. The highest intensity of (111) peaks in film deposited under 50 mL/min gas flow rate may be related with the highest N and C concentration and good crystallinity of nitride and carbide. The crystal size of Ti(C, N, O) crystal in (111) plane increases from 6.4 nm (10 mL/min) to 12.5 nm (50 mL/min). There is not any peak in 70 and 80 mL/min gas flow rate, which implies an amorphous TiO_2 structure. When gas flow rate is high (≥70 mL/min), the ratio of O/Ti is

higher than 1 (Fig.2). Because of high standard enthalpy of TiO$_2$ (TiO$_2$:-672 kJ mol^{-1}, TiO:-520 kJ mol^{-1}, TiN:-338 kJ mol^{-1}, TiC:-184 kJ mol^{-1}), Ti is preferentially consumed by O to develop amorphous TiO$_2$ phase.

2.2.3 Raman results

Raman spectroscopy is a useful tool for characterizing the structural arrangement of amorphous carbon. As shown in Fig.6, the peak around 1575 cm^{-1} corresponding to G peak, originates from lattice vibrations in the plane of the graphite-like rings, and the peak around 1350 cm^{-1}, corresponding to D peak, is due to the disorder-allowed zone edge mode of graphite [12]. There are apparent D and G peaks corresponding to amorphous carbon phase in films deposited under 50 and 80 mL/min gas flow rate. Therefore, the films deposited under lower gas flow rate (≤30 mL/min) are composed of single solid soluted Ti(C, N, O) nanocrystal. While Film deposited under 50 mL/min is composed of nc-Ti(C,N,O)/a-CN$_x$ nanocomposite, and the films deposited under higher gas flow rate are composed of a-TiO$_2$/a-CN$_x$ (70 mL/min) or N-doped a-TiO$_2$/a-C (80 mL/min).

2.3 Internal stress, friction and anti-corrosion behavior

2.3.1 Internal stress

Fig.7a shows the internal stress of films as a function of gas flow rate. The internal stress of films deposited under 10 and 30 mL/min gas flow rate is higher than 4 GPa. The reason is the "atomic peening" effect of Ti ions with high energy under low gas pressure (≤30 mL/min), which can lead to high compressive stress in films[13]. Another reason may also be related with the high elastic modulus of nc-Ti(C, N, O) structure, which leads to the difficulty for the stress relief. The decreasing internal stress under 50 mL/min is connected to the existence of C and CN$_x$ amorphous phase, which can release stress. The totally amorphous phase structures and weak "atomic peening" effect under high gas flow rate (≥70 mL/min) contribute to the lowest internal stress of films deposited under 70 and 80 mL/min gas flow rate.

2.3.2 Friction coefficient

The average friction coefficients of films deposited under different gas flow rates are shown in Fig.7b. The average friction coefficients of single Ti(C, N, O) nanocrystal films deposited under 10 to 50 mL/min gas flow rate are about 0.7, and the nc-Ti(C, N, O) crystals in films may enhance the frictional resistance. Though there is a little amorphous carbon in nc-Ti(C, N, O)/a-CN$_x$ nanocomposite film deposited under 50 mL/min gas flow rate, the average friction coefficient of the film is the highest (~0.8). As phase structure transforms to N-doped a-TiO$_2$/a-C (80 mL/min) amorphous structure, the average friction coefficient of N-doped a-TiO$_2$/a-C film (80 mL/min) decreases to 0.34. Amorphous TiO$_2$ films show low friction coefficient[14], carbon amorphous phase possesses self-lubricant function[15],
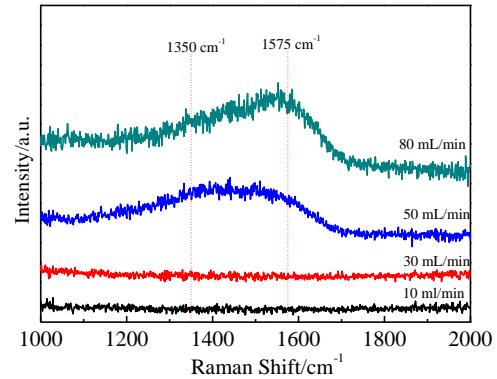

Fig.6   Raman spectra of films deposited under 50 and 80 mL/min CO$_2$ and N$_2$ gas mixture flow rate
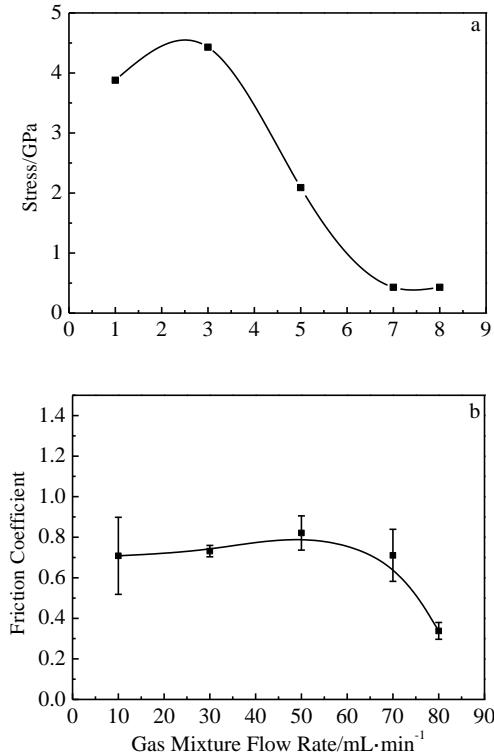

Fig.7   Internal stress (a) and average friction coefficient (b) of the films deposited under different gas mixture flow rate

so the combination amorphous TiO$_2$ and carbon may contribute to the lowest friction coefficient of film deposited under 80 mL/min gas flow rate.

2.3.3 Anti-corrosion property

Potentiodynamic polarization curves of films deposited on 304 SS substrates under different gas flow rates and bare 304 SS substrate are plotted in Fig.8. The corrosion current density (I_{corr}) and corrosion potential (E_{corr}) are determined from the Tafel curve by the extrapolation method. The

corrosion polarization resistance (R_p) is calculated using the Tafel-extrapolation method and the following equation:

$$R_p = \frac{b_a b_c}{2.303 I_{corr}(b_a + b_c)} \quad (3)$$

where, b_a, b_c are anodic/cathodic Tafel slope. As shown in Fig.8, all the nc-Ti(C, O, N) nanocrystal structure (10 mL/min), nc-Ti(C, O, N)/a-CN$_x$ nanocomposite structure (50 mL/min) and N-doped a-TiO$_2$/a-C nanocomposite structure (80 mL/min) show obvious passivation phenomena and apparent enhancement of pitting potential (when I_{corr} =20 μA/cm^2), which indicates a good corrosion protective function of films. As shown in Table 2, N-doped a-TiO$_2$/a-C amorphous structure under 80 mL/min gas flow rate possesses the lowest I_{corr}, passivating current density and highest R_p, the corrosion rate is reduced to 40% comparing with bare 304 SS, which indicates good corrosion protective ability. The corrosion protective mechanism of N-doped
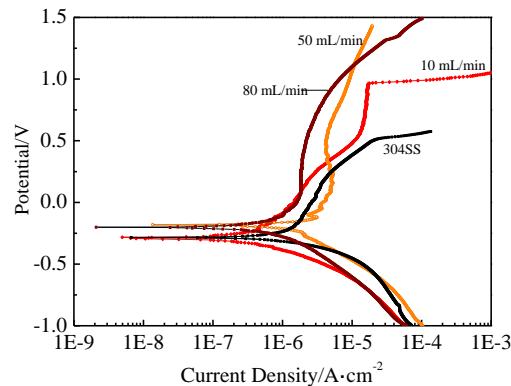

Fig.8 Potentiodynamic polarization curves of films deposited on 304 SS substrates

Table 2 Parameters from potentiodynamic polarization curves of the films deposited under different gas mixture flow rates and 304 SS

CO_2 gas flow rate/ mL·min^{-1}	Phase structure	Corrosion current density/μA cm^{-2}	Corrosion voltage/V	R_p/ kΩ cm^2	Pitting potential/V	Corrosion rate/μm a^{-1}
10	nc-Ti(C,N,O)	0.32	-0.28	18	0.97	3.8
50	nc-Ti(C,N,O) /a-CN$_x$	0.48	-0.18	23	1.45	9.1
80	N-doped a-TiO$_2$/a-C	0.17	-0.20	105	1.24	2.0
304SS	-	0.44	-0.29	40	0.50	5.2

a-TiO$_2$/a-C films may be the low electrical conductivity of the a-TiO$_2$ phase and the presence of carbon amorphous phases in films hampering the electron transport and the exchange of the electrical charges at films surface, which is necessary for the electrochemical corrosion[16]. Thus, Ti(C, O, N) nano- composite films act as inert physical barriers to the initiation and development of corrosion process.

3 Conclusions

1) Ti(C,N,O) nanocomposite films are successfully fabricated by FCVA technique using CO_2 and N_2 (1:1) as reactive gas. The contents of C and N increase obviously, while contents of O and Ti decrease slightly as the gas flow rate increases from 10 to 50 mL/min, and the contents of C and N decrease while content of Ti increase slightly and content of O increase dramatically as the gas flow rate increases from 50 to 80 mL/min. The structure of films transforms through nc-Ti(C, N, O) nanocrystal, nc-Ti(C, N, O)/a-CN$_x$ nanocomposite to a-TiO$_2$/a-CN$_x$ and N-doped a-TiO$_2$/a-C nanocomposite as gas flow rate rises from 10 to 80 mL/min. N-doped a-TiO$_2$/a-C nanocomposite shows the lowest average friction coefficient (0.34).

2) Both nc-Ti(C,N,O)/a-C/a-CN$_x$ and N-doped a-TiO$_2$/a-C nanocomposite show good corrosion resistance in Hanks balanced solution, implying a great potential in medical application. The remarkable effect of gas flow rate on

structure, tribological performance and anti-corrosion properties of Ti(C, N, O) films offers feasible process to tailor the films on need.

References

1 Ghareshabani E, Rawat R S, Sobhanian S *et al. Nuclear Instruments and Methods in Physics Research B*[J], 2010, 268(17): 2777

2 Zhang Guojun, Li Bin, Jiang Bailing *et al. Journal of Materials Science Technology*[J], 2010, 26(2): 119

3 Zhang Lin, Ma Guojia, Ma He *et al. Nuclear Instruments and Methods in Physics Research B*[J], 2014, 333: 1

4 Chappe J M, Vaz F, Cunha L *et al. Surface & Coating Technology*[J], 2008, 203(5): 804

5 Fouad O A, Geioushy R A, EI-Sheikh S M *et al. Journal of Alloys and Compounds*[J], 2011, 509(20): 6090

6 Zhou F Z, Fu K H, Liao B *et al. Applied Surface Science*[J], 2015, 327: 350

7 Wang Y H, Zhang X, Wu X Y *et al. Applied Surface Science*[J], 2008, 254(16): 5085

8 Zhao Z W, Tay B K. *Journal of Applied Physics*[J], 2007, 101: 1

9 Chappe J M, Fernandes A C, Moura C *et al. Surface and Coatings Technology*[J], 2012, 206(8): 2525

10 Guillot J, Fabreguette F, Imhoff L *et al. Applied Surface Science*[J], 2001, 177(4): 268

11 Sobczyk-Guzenda A, Pietrzyk B, Jakubowski W *et al. Materials Research Bulletin*[J], 2013, 48(10): 4022

12 Wood R M, Edwards A K, Steuer M F *et al. Journal of Chemical Physics*[J], 1980, 73(8): 3709

13 Zhu D Y, Zheng C X, Chen D H *et al. Plasma Science and Technology*[J], 2013, 15(11): 1116

14 Jia Q Y, Zhang Y J, Wu Z S *et al. Tribology Letters*[J], 2007, 26(1): 19

15 Li D J, Hassanni S, Poulin S *et al. Journal of Applied Physics*[J], 2012, 111: 4

16 Sui J H, Gao Z Y, Cai W *et al. Materials Science and Engineering A, Structural Materials Properties Microstructure Materials Properties*[J], 2007, 454: 472

使用磁过滤阴极弧法以 CO_2 和 N_2 为反应气体制备 Ti(C,N,O)纳米复合薄膜的研究

侯庆艳，沈永青，伏开虎，周 晗，英敏菊，张 旭，廖 斌

(北京师范大学 射线束技术与材料改性教育部重点实验室，北京 100875)

摘 要：使用磁过滤阴极弧法（FCVA）以 CO_2 和 N_2 为反应气体在 Si（100）和 304 不锈钢衬底上沉积 Ti(C,N,O)纳米复合薄膜，CO_2 和 N_2 流量比为 1;1。薄膜的成分、结构和性能分别采用 XPS、XRD、Raman、SEM、摩擦磨损试验机和电化学实验站检测得出。当混合气体流量从 10 mL/min 增加到 50 mL/min 时，薄膜中的 C 和 N 含量有明显增加，而 O 和 Ti 含量有小幅下降；当混合气体流量从 50 mL/min 增加到 80 mL/min 时，薄膜中的 C 和 N 含量下降，而 Ti 含量有小幅上升，O 含量急剧上升。薄膜由 nc-Ti(C,N,O)纳米晶结构转变为 nc-Ti(C,N,O)/a-CN_x，a-TiO_2/a-CN_x 和 N-doped a-TiO_2/a-C 纳米复合结构。N-doped a-TiO_2/a-C 纳米复合结构薄膜具有最低的摩擦系数（0.34），nc-Ti(C,N,O)/a-CN_x 和 N-doped a-TiO_2/a-C 纳米复合结构薄膜在 Hanks 溶液中均表现出良好的抗腐蚀能力。

关键词：Ti(C,N,O)；磁过滤阴极弧；CO_2腐蚀；纳米复合

作者简介：侯庆艳，女，1990 年生，硕士生，北京师范大学核科学与技术学院，北京 100875，电话：010-62208249, E-mail: www-hqy@163.com